WALAILAK JOURNAL
http://wjst.wu.ac.th Engineering and Physical Sciences

Entropy Analysis for Unsteady MHD Boundary Layer Flow and Heat Transfer of Casson Fluid over a Stretching Sheet

Mohamed Ahmed MANSOUR[1], Abd Elnaser Sobhy Mohamed MAHDY[2], Sameh Elsayed AHMED[2] and Shadia Saber MOHAMED[2,*]

[1]*Mathematics Department, Faculty of Sciences, Assiut University, Assiut, Egypt*
[2]*Mathematics Department, Faculty of Sciences, South Valley University, Qena, Egypt*

([*]Corresponding author's e-mail: shadia_saber@yahoo.com)

Received: 17 June 2015, Revised: 26 April 2016, Accepted: 18 May 2016

Abstract

This paper investigates the entropy generation analysis of the unsteady two-dimensional magnetohydrodynamic (MHD) flow of electrically conducting non-Newtonian Casson fluid and heat transfer towards a stretching sheet in the presence of uniform transverse magnetic field with viscous dissipation and Joule heating effects. Using similarity solutions, the governing partial differential equations are transformed into ordinary differential equations and then solved numerically by MATLAB function *bvp4c*. The results of the present study indicate that the flow and temperature fields are significantly influenced by unsteadiness parameter A, Casson parameter β, magnetic parameter M, Prandtl number Pr, and Eckert number Ec. It is found that the fluid velocity initially decreases with increase in the unsteadiness parameter A, and that temperature decreases significantly due to the unsteadiness parameter. Also, the effect of increasing values of the Casson parameter β is to suppress the velocity field and the temperature distributions. The influences of the same parameters, as well as the Reynolds number and the Brinkman number on the entropy generation, are also discussed.

Keywords: Entropy, MHD, Casson fluid, stretching sheet, viscous dissipation

Introduction

In fluid dynamics, the effects of external magnetic field on magnetohydrodynamic (MHD) flow over a stretching sheet are very important due to its applications in many engineering problems, such as glass manufacturing, geophysics, paper production, and the purification of crude oil. Crane [1], firstly, considered the steady laminar boundary layer flow of a Newtonian fluid caused by a linearly stretching sheet. His investigations helped to form the boundary layer theory and the uniqueness of solutions and pioneered many fields. Sakiadis [2,3] reported on a flow field analysis where the stretched surface was assumed to move with uniform velocity, and similarity solutions were obtained for the governing equations. The solution was later improved by Howarth [4]. Gupta and Gupta [5] studied the effect of mass transfer on a stretching sheet with suction or blowing for linear surface velocity subject to a uniform temperature. Wang [6] investigated the three-dimensional flow due to the stretching surface. Mishra and Jena [7] studied the numerical solution of MHD boundary layer flow with viscous dissipation. In all these studies, the flow and temperature fields were considered to be at a steady state. However, in some cases, the flow field, heat and mass transfer can be unsteady, due to studding, stretching of the flat sheet, or by a step change of the sheet temperature. A few papers have been published on the boundary layer flow and heat transfer problems where the stretching force and surface temperature vary with time. Some authors[8-10] studied the problem of unsteady isothermal stretching surface by using similarity variables

to transform the governing time-dependent boundary layer equations into a set of ordinary differential equations. Elbashbeshy and Bazid [11] presented similarity solutions of the boundary layer equations that describe the unsteady flow and heat transfer over an unsteady stretching sheet. Sharidan *et al.* [12] studied the unsteady flow and heat transfer over a stretching sheet in a viscous and incompressible fluid. Recently, Ishak *et al.* [13], Mukhopadhyay [14,15], and Chamkha *et al.* [16] obtained similarity solutions for unsteady flow and heat transfer over a stretching sheet under different conditions. Hayat *et al.* [17] analyzed the time-dependent flow over a stretching surface. Mukhopadhyay and Gorla [18] analyzed the effects of slip on unsteady boundary layer stagnation point flow past a stretching sheet. Of late, Hayat *et al.* [19] discussed the three-dimensional flow of Jeffery fluid past a stretching surface.

In all the investigations mentioned above, classical Newtonian fluids are discussed. However, models [20,21] have been proposed to clarify all the physical behaviors of Casson fluid. Casson fluid is one of the types of such non-Newtonian fluids which behave like these fluid models and have their origin in the modeling of flow of many biological fluids, especially blood. It is considered, also, a good approximation for many other materials, such as foams, yoghurt, molten chocolate cosmetics, nail polish, tomato purée, some particulate suspensions inelastic solids, etc. For this fluid, a yield shear stress exists in the constitutive equation. The unsteady boundary layer flow and heat transfer of a Casson fluid over a moving flat plate with a parallel free stream were studied by Mustafa *et al.* [21]. They solved the problem analytically, using the homotopy analysis method (HAM). Recently Mukhopadhyay *et al.* [22] discussed Casson fluid flow over an unsteady stretching surface. Bhattacharyya *et al.* [23,24] reported the exact solution for boundary layer flow of Casson fluid over a permeable stretching/shrinking sheet, with and without external magnetic field. Qasima *et al.* [25] investigated the heat transfer in the boundary layer flow of a Casson fluid over a permeable shrinking sheet with viscous dissipation.

Physically, entropy generation is associated with thermo dynamical irreversibility, which is a common phenomenon in all kinds of heat transfer designs. A Greater rate of entropy generation in any thermal system destroys the useful work of, and greatly reduces the efficiency of, the system. Bejan [26,27] presented a method named Entropy Generation Minimization (EGM) to measure and optimize the disorder or disorganization generated during a process, specifically in the fields of refrigeration (cryogenics), heat transfer, storage, and solar thermal power conversion. The entropy generation analysis of nanofluids was investigated by Mahian *et al.* [28]. It is important to note that the second law of thermodynamics is more reliable than the first law of thermodynamics analysis because of the limitation of the first law efficiency in a heat transfer engineering systems (Oztop and Al-Salem [29]), and, also, that heat transfer, mass transfer, viscous dissipation, etc., can be used as the sources of entropy generation. Aïboud and Saouli [30,31] analyzed entropy generation for viscoelastic magneto hydrodynamic flow over a stretching surface. They illustrated that the entropy generation number increases for high magnetic parameters. Recently Govindaraju *et al.* [32] studied the entropy generation analysis for MHD flow of a nanofluid over a stretching sheet. They observed that the entropy generation depends on the thermal conductivity of the nanoparticles which are presented in the base fluid. The entropy generation is high for metallic nanofluids and is low for non-metallic nanofluids. Abolbashari *et al.* [33] investigated the problem of entropy analysis in an unsteady magnetohydrodynamic flow and the heat transfer of the water as the base nanofluid and four different types of nanoparticles over a stretching permeable surface using the HAM. Rashidi *et al.* [34] used HAM to discuss the entropy generation of the revised Cheng-Minkowycz problem, which presents the problem of natural convection and boundary layer flow of a nanofluid through a porous medium. They observed that the increase in the irreversibility distribution ratios leads to increase in the values of entropy. Rashidi *et al.* [35] performed the effects of variable properties on the entropy generation in MHD flow over a rotating porous disk using the fourth-order Runge-Kutta method. Their results show that the average entropy generation decreases as the magnetic field parameter, temperature difference parameter, or suction parameter increases. HAM was applied by Abolbashari *et al.* [36] to discuss the entropy generation for Casson nanofluid flow past a stretching sheet. They found that the entropy generation number can be enhanced by increase in thermophoresis parameter, Biot number, or the Brownian motion parameter.

The main objective of this study is to investigate the effects of viscous dissipation and Joule heating on the entropy generation due to unsteady MHD mixed convection flow of a Casson fluid over a

stretching sheet. The similarity solutions are obtained and the reduced ordinary differential equations are solved numerically using MATLAB software. The variations in physical characteristics of the flow dynamics and heat transfer for several parameters involved in the equations are discussed in detail. The influences of the governing parameters on the entropy generation are also discussed.

Materials and methods

Flow analysis

Consider a laminar boundary layer two-dimensional flow and heat transfer of an incompressible, conducting non-Newtonian Casson fluid over an unsteady stretching sheet. The unsteady fluid and heat flows start at $t = 0$. The sheet emerges out of a slit at origin $(x = 0, y = 0)$ and moves with non-uniform velocity $U_w(x,t) = cx/(1-\alpha t)$ where $c > 0$, $\alpha \geq 0$ are constants with dimensions $(time)^{-1}$ and *c* is the initial stretching rate. The heat transfer in the presence of viscous dissipation and Joule heating effects is also taken into account. The rheological equation of state for an isotropic and incompressible flow of a Casson fluid is (see Mukhopadhyay *et al*. [22]);

$$\tau_{ij} = \begin{cases} 2(\mu_B + p_y/\sqrt{2\pi})e_{ij}, & \pi > \pi_c \\ 2(\mu_B + p_y/\sqrt{2\pi_c})e_{ij}, & \pi < \pi_c \end{cases} \tag{1}$$

In the above equation $\pi = e_{ij}e_{ij}$ and e_{ij} is the $(i, j)^{\text{th}}$ components of the deformation rate, π_c is a critical value of this product based on the non-Newtonian model, π_B is the dynamic viscosity of the non-Newtonian fluid, and p_y is the yield stress of fluid. The boundary layer equations with viscous dissipation can be written, per Sharidan *et al.* [12] and Chamakha *et al*. [16] as;

$$\frac{\partial u}{\partial x} + \frac{\partial v}{\partial y} = 0 \tag{2}$$

$$\frac{\partial u}{\partial t} + u\frac{\partial u}{\partial x} + v\frac{\partial v}{\partial y} = \upsilon(1+1/\beta)\frac{\partial^2 u}{\partial y^2} - \frac{\sigma B_0{}^2 u}{\rho}, \tag{3}$$

$$\frac{\partial T}{\partial t} + u\frac{\partial T}{\partial x} + v\frac{\partial T}{\partial y} = \frac{k}{\rho c_p}\frac{\partial^2 T}{\partial y^2} + \frac{Q_0}{\rho c_p}(T - T_\infty) + \frac{\mu}{\rho c_p}(1+1/\beta)\left(\frac{\partial u}{\partial y}\right)^2 + \frac{\sigma B_0{}^2 u^2}{\rho c_p}. \tag{4}$$

where u and v are the velocity components in the x -and y -components, $\beta = \mu_B\sqrt{2\pi_c}/Py$ is the Casson fluid parameter, σ is the electrical conductivity of the fluid, B_0 is the strength of magnetic field applied in the y direction, T is the fluid temperature, T_∞ is the free stream temperature, k is the thermal conductivity of the fluid, c_p is the specific heat, $\upsilon = (\mu/\rho)$ is the kinematic viscosity, ρ is the density of the fluid, and Q_0 is the volumetric of heat generation or absorption.

Boundary conditions

The appropriate boundary conditions for the problem are given by;

$$u = U_{w,}\ v\ = -v_w\ , T\ = T_w at\ y\ = 0, \tag{5}$$

$$u \to 0, T\ \to T_\infty as\ y\ \to \infty. \tag{6}$$

where v_w is the wall mass transfer velocity, with $v_w > 0$ for mass suction and $v_w < 0$ for mass injection. $T_w(x,t) = T_\infty + cx^2 T_0\ (1-\alpha t)^{-\frac{3}{2}} / 2\upsilon$ (see [9]), where T_0 is a (positive or negative; heating or cooling) reference temperature (slit temperature at $x = 0$, T_∞ is the constant free stream temperature). The expressions for $U_w(x,t), T_w(x,t)$ are valid for time $t < \alpha^{-1}$.

Method of solution

In this section, we introduce the stream function ψ as;

$$u = \frac{\partial \psi}{\partial y}, v\ = -\frac{\partial \psi}{\partial x} \tag{7}$$

and define the following variables;

$$\psi = \sqrt{c\upsilon/(1-\alpha t)}x\ f\ (\eta),\ \eta = y\sqrt{\frac{c}{\upsilon(1-\alpha t)}},\ \theta(\eta) = \frac{T\ -T_\infty}{T_w\ -T_\infty} \tag{8}$$

and

$$T_w(x,t) = T_\infty + cx^2 T_0 (1-\alpha t)^{-\frac{3}{2}} / 2\upsilon \tag{9}$$

Now, equations (3) and (4) can be written as;

$$A\ (\frac{\eta}{2}f'' + f') + (1+1/\beta)f''' + f\ f'' - f'^2 - Mf' = 0, \tag{10}$$

$$\frac{A}{2}(\eta\theta' + 3\theta) + \theta'' + \Pr\left(f\ \theta' + \lambda\theta + (1+1/\beta)Ecf''^2 + MEcf'^2\right) = 0, \tag{11}$$

where $A = \frac{\alpha}{c}$ is the unsteadiness parameter, $M = \sigma_e B_0^{\ 2}(1-\alpha t)/\rho c$ is the magnetic parameter and $Ec = U_w^2 / c_p\left(T_w - T_\infty\right)$ is the Eckert number, $\Pr = \mu c_p / k$ is the Prandtl number and $\lambda = Q_0 / \rho c_p c$ is the heat source $(\lambda < 0)$ or sink parameter $(\lambda > 0)$.

The converted boundary conditions are written as follows;

$$f(\eta) = S, f'(\eta) = 1, \theta = 1 at\ \eta = 0 \tag{12}$$

$$f'(\eta) \to 0; \theta(\eta) \to 0 as\ \eta \to \infty. \tag{13}$$

where $S = v_w / (c\upsilon)^{1/2}$ is the wall mass transfer parameter.

The physical quantities of interest in the problem are the skin–friction coefficient C_f and the local Nusselt number Nu_x, which can be expressed, respectively, as;

$$C_f = \frac{\left(\mu_B + p_y / \sqrt{2\pi}_c\right)\left(\frac{\partial u}{\partial y}\right)_{y=0}}{\rho U_w{}^2} = \sqrt{\mathrm{Re}_x}\,(1+1/\beta) f''(0), \tag{14}$$

$$N_u = \frac{x\left(\frac{\partial T}{\partial y}\right)_{y=0}}{(T_w - T_\infty)} = -\sqrt{\mathrm{Re}_x}\,\theta'(0), \tag{15}$$

where $\mathrm{Re}_x = \frac{U_W x}{\upsilon(1-\alpha t)}$ is the Reynolds number based on the stretching velocity $U_W(x)$.

Entropy generation analysis

According to Woods [33], the local volumetric rate of entropy generation in the presence of a magnetic field is given by;

$$S_G = \frac{k}{T_\infty^2}\left(\frac{\partial T}{\partial y}\right)^2 + \frac{\mu(1+1/\beta)}{T_\infty}\left(\frac{\partial u}{\partial y}\right)^2 + \frac{1}{T_\infty}\sigma B_0^2 u^2 \tag{16}$$

Eq. (16) clearly shows the contributions of 3 sources of entropy generation. The first term on the right-hand side of Eq. (16) is the entropy generation due to heat transfer across finite temperature difference; the second term is the local entropy generation due to viscous dissipation, whereas the third term is the local entropy generation due to the effect of the magnetic field. It is appropriate to define the dimensionless number for entropy generation rate Ns. This number is defined by ratio of the local volumetric entropy generation rate S_G to a characteristic entropy generation rate S_{G0}. For a prescribed boundary condition, the characteristic entropy generation rate is;

$$S_{G0} = \frac{k(\Delta T)^2}{l^2 T^2{}_\infty} \tag{17}$$

where T_∞ is a reference temperature and l is the characteristic length. Therefore, the entropy generation number is;

$$Ns = \frac{S_G}{S_{G0}} \tag{18}$$

By applying the similarity transformations in Eq. (16), the entropy generation number is given by;

$$Ns = \mathrm{Re}_l \left(\frac{\partial \theta}{\partial y}\right)^2 + \mathrm{Re}_l \frac{Br}{\Omega}\left[\left(M^2 u^2\right) + (1+1/\beta)\left(\frac{\partial u}{\partial y}\right)^2\right] \tag{19}$$

where Br is the Brinkman number, Re_l is the Reynolds number based on the characteristic length, and Ω is the dimensionless temperature difference. These parameters are given by the following relationships;

$$Br = \frac{\mu U_w^2}{k(\Delta T)},\ \mathrm{Re}_l = \frac{U_l l}{\upsilon},\ \Omega = \frac{T_w - T_\infty}{T_\infty} \tag{20}$$

Numerical procedure

In order to solve the ordinary differential equations (ODEs), Eqs. (10) and (11), with the boundary conditions Eqs. (12) and (13) using MATLAB software, the following technique is presented;

Step 1: The new variables are defined;

$$Y_1 = f, Y_2 = f', Y_3 = f'', Y_4 = \theta, Y_5 = \theta' \tag{21}$$

Using Eq. (21), the system of ODEs Eqs. (10) and (11) is converted to the following large system of first-order ODEs;

$$\frac{dY_1}{d\eta} = Y_2(\eta) \tag{22}$$

$$\frac{dY_2}{d\eta} = Y_3(\eta) \tag{23}$$

$$\frac{dY_3}{d\eta} = \frac{\left[MY_2 + Y_2^2 - Y_1 Y_3 - A\left(\frac{\eta}{2}Y_3 + Y_2\right)\right]}{\left[1+\frac{1}{\beta}\right]} \tag{24}$$

$$\frac{dY_4}{d\eta} = Y_5(\eta) \tag{25}$$

$$\frac{dY_5}{d\eta} = -\Pr\left(Y_1 Y_5 + \lambda Y_4 + \left(1+\frac{1}{\beta}\right)EcY_3^2 + MEcY_2^2\right) - \frac{A}{2}(\eta Y_5 + 3Y_4) \tag{26}$$

The boundary conditions Eqs. (12) and (13) are also converted to;

$$y_1(0) = S, y_2(0) = 1, y_4(0) = 1, y_2(\eta_{max}) = 0, y_4(\eta_{max}) = 0 \tag{27}$$

Step 2: The function *bvp4c* is recalled from the MATLAB library to solve the previous first-order ODEs;

Here, the value of η_{max} is considered to be equal to 15, whereas, the step size $\Delta\eta$ is considered to be equal to 0.03. In order to validate the method used in this study, and to judge the accuracy of the present analysis, a comparison with available results corresponding to the skin-friction coefficient $f''(0)$ for the unsteady flow of viscous incompressible Newtonian fluid are compared with the available results of Sharidan *et al.* [12], Chamkha *et al.* [16] and Mukhopadhyay *et al.* [22]. As can be observed from **Table 1**, there are excellent agreements between the results.

Table1 The values of $f''(0)$ for various values of unsteadiness parameter A with $\beta = 0$.

A	Sharidan *et al.* [12]	Chamakha *et al.* [16]	Mukhopadhyay *et al.* [22]	Present study
0.8	-1.261042	-1.261512	-1.261479	-1.2615010
1.2	-1.377722	-1.378052	-1.377850	-1.377130

Results and discussion

Numerical computations are performed for various values of the physical parameters involved, i.e., unsteadiness parameter $(0.6 \le A \le 2)$, Casson parameter $(0.1 \le \beta < \infty)$, magnetic parameter $(1.0 \le M \le 10)$, mass suction parameter $(-3 \le S \le 3)$, Prandtl number $(0.1 \le Pr \le 5)$, Eckert number $(0.1 \le Ec \le 5)$, and heat (source/sink) parameter $(-0.25 \le \lambda \le 0.25)$. In addition, the same parameters, as well as the Reynolds number $(10 \le \mathrm{Re}_l \le 70)$, and the dimensionless group parameter $(10 \le Br/\Omega \le 70)$ on the entropy generation are discussed.

Figure 1 exhibits the velocity profiles for several values of the unsteadiness parameter A. It is seen that the velocity along the sheet decreases initially with the increase in the unsteadiness parameter A, and this implies an accompanying reduction of the momentum boundary layer thickness near the wall. **Figure 2** represents the effects of unsteadiness parameter *A* on the temperature distributions. From this figure, it is noticed that the temperature at a particular point decreases significantly with increase in the unsteadiness parameter. The effects of Casson parameter β on the velocity and temperature profiles for unsteady motion are clearly exhibited in **Figures 3** and **4**, respectively.

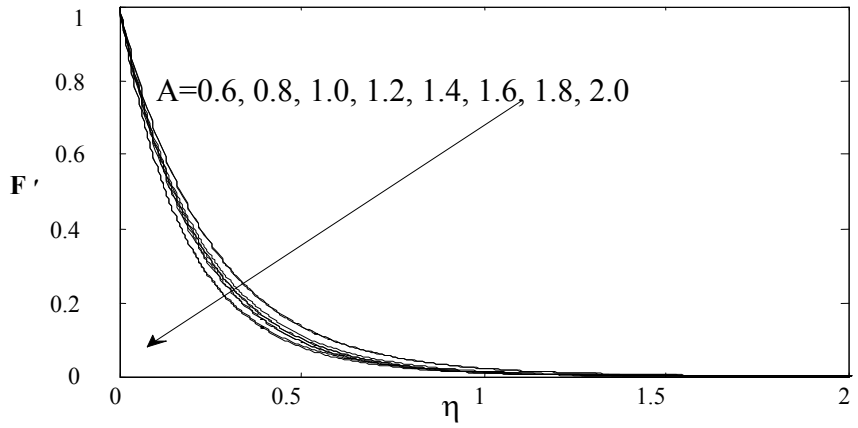

Figure 1 Effects of A on $f'(\eta)$ at $S = 2.0$, M = 1.0, Ec = 0.1, β=5.0, Pr = 0.71, $\lambda = -2.0$.

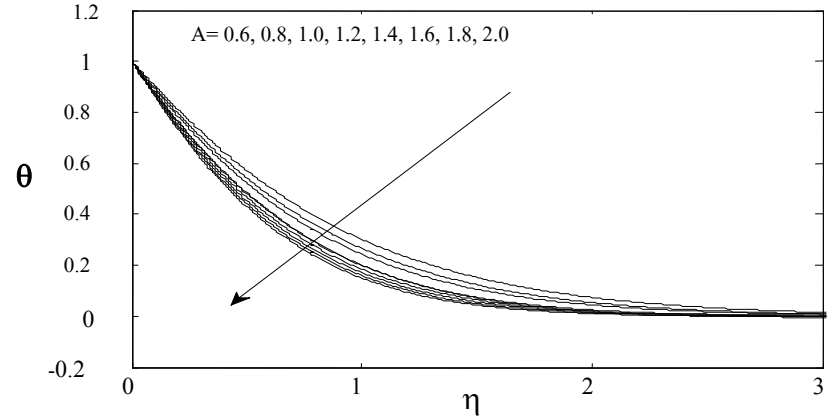

Figure 2 Effects of A on $\theta(\eta)$ at $S = 2.0$, M =1.0, Ec = 0.1, β=5.0, Pr = 0.71, $\lambda = -2.0$.

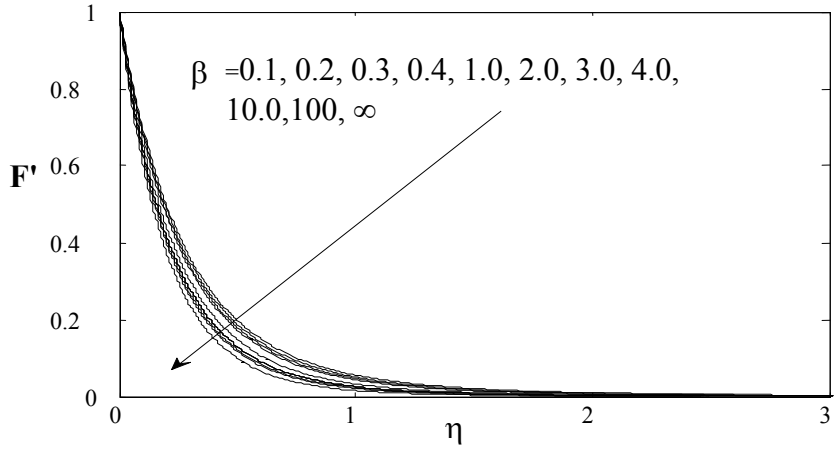

Figure 3 Effects of β on $f'(\eta)$ at $S = 2.0$, M =1.0, Ec = 0.1, A = 5.0, Pr = 0.71, $\lambda = -2.0$.

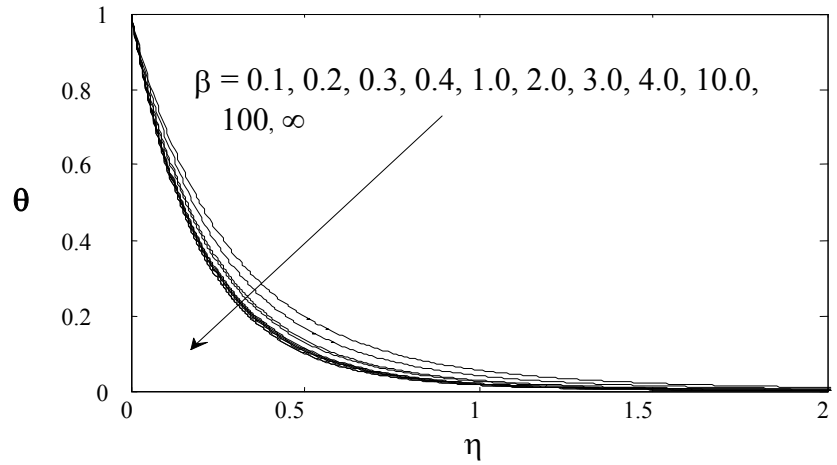

Figure 4 Effects of β on $\theta(\eta)$ at $S = 2.0$, M =1.0, Ec = 0.1, A = 5.0, $\Pr = 0.71, \lambda = -2.0$.

The same type of behavior of velocity with increasing β is noted. The effect of increasing values of β causes a reduction in profiles of the velocity and, hence, the boundary layer thickness decreases. The increasing values of the Casson parameter, i.e., the decreasing yield stress (the fluid behaves as a Newtonian fluid as the Casson parameter becomes large), suppress the velocity field. It can be concluded that $f'(\eta)$, and that the associated boundary layer thickness leads to decreasing function in β. **Figure 4** shows that the increase in β leads to reduction in the temperature field for the unsteady motion. **Figures 5** and **6** display the effect of variation of magnetic field parameter M on the fluid velocity and temperature distributions, respectively. Due to the increase of the magnetic parameter, the dimensionless velocity at fixed η decreases, and the boundary layer thickness decreases. This can be attributed to the Lorentz force induced by the dual actions of electric and magnetic fields that reduces the velocity and increases the temperature.

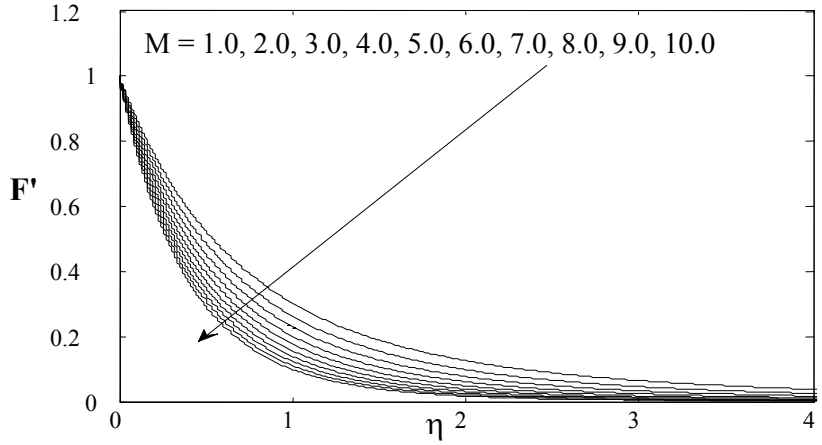

Figure 5 Effects of M on $f'(\eta)$ at $S = 2.0$, β = 5.0, Ec = 0.1, A = 5.0, $\Pr = 0.71, \lambda = -2.0$.

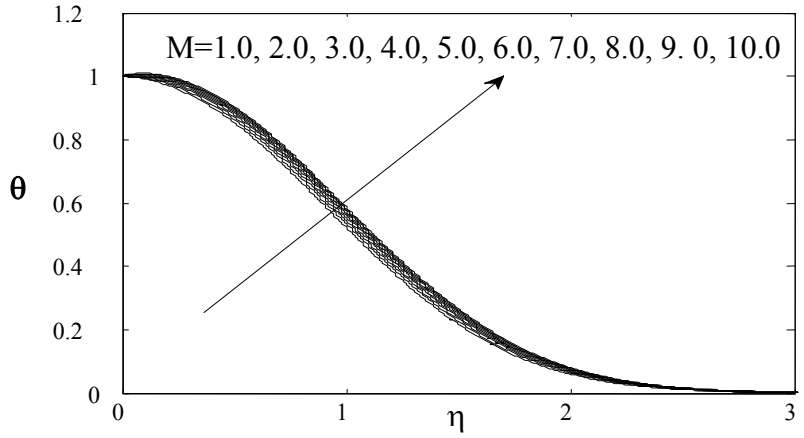

Figure 6 Effects of M on $\theta(\eta)$ at $S = 2.0$, $\beta = 5.0$, $Ec = 0.1$, $A = 5.0$, $\Pr = 0.71$, $\lambda = -2.0$.

Figure 7 depicts the effect of suction/injection parameter *S* on the velocity profiles. It is observed that, by increasing the values of the suction parameter, the velocity decreases. **Figure 8** shows the effects of *S* on the temperature distributions $\theta(\eta)$. It is observed that, for any fixed value of η, the temperature decreases as *S* increases. The temperature profiles for various values of the heat source or sink parameter λ are exhibited in **Figure 9**. It is noted that, for a fixed value of η, temperature decreases as λ increases. The dimensionless temperature profiles $\theta(\eta)$ for several values of Prandtl Number $\Pr$ are represented in **Figure 10**. It is found that the temperature distributions decrease with the increasing of Pr. **Figure 11** shows the effect of Ec on the temperature distributions. It is noted that an increase in Eckert number Ec reduces the temperature distributions $\theta(\eta)$. The variations of skin-friction coefficient $f''(0)$ and the heat transfer coefficient $\theta'(\eta)$ versus the unsteadiness parameter A for various values of β, Ec and $\Pr$ are presented in **Figures 12 - 15**.

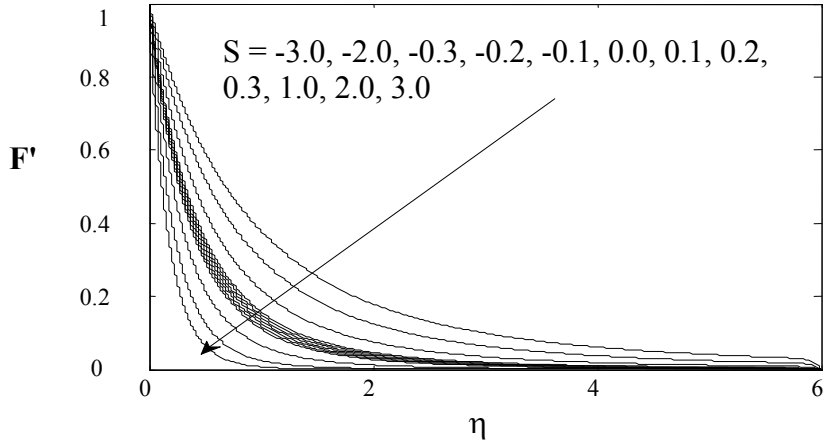

Figure 7 Effects of S on $f'(\eta)$ at $M = 1.0$, $\beta = 5.0$, $Ec = 0.1$, $A = 5.0$, $\Pr = 0.71$, $\lambda = -2.0$.

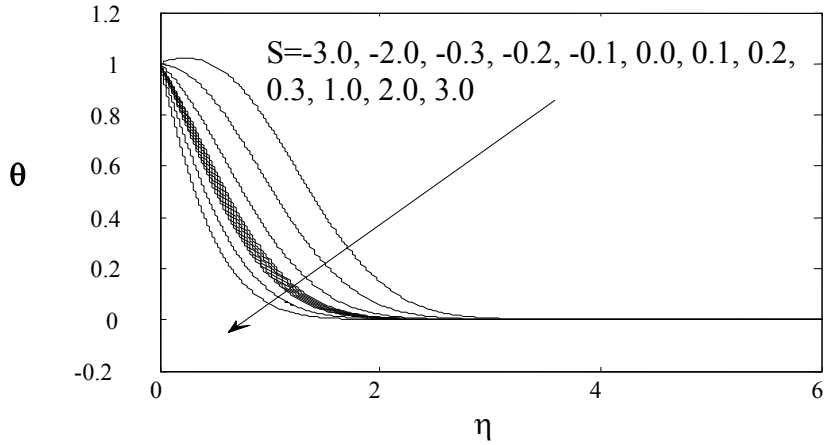

Figure 8 Effects of S on $\theta(\eta)$ at $M = 1.0$, $\beta = 5.0$, $Ec = 0.1$, $A = 5.0$, $\Pr = 0.71$, $\lambda = -2.0$.

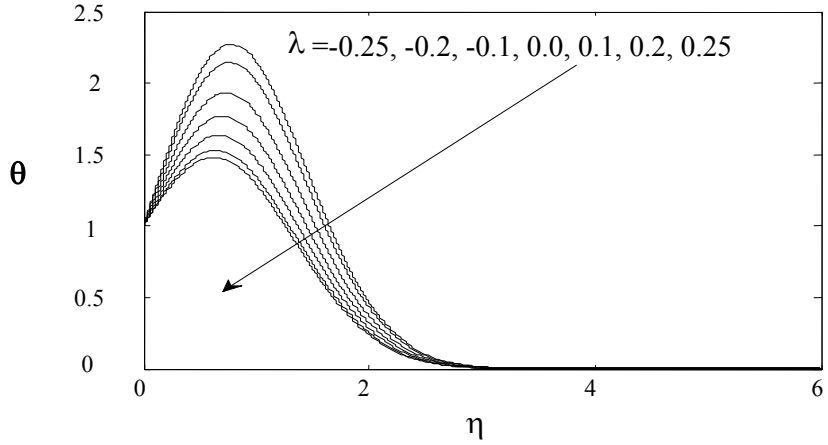

Figure 9 Effects of λ on $\theta(\eta)$ at $M = 1.0$, $\beta = 5.0$, $Ec = 0.1$, $A = 5.0$, $\Pr = 0.71$, $S = 2.0$.

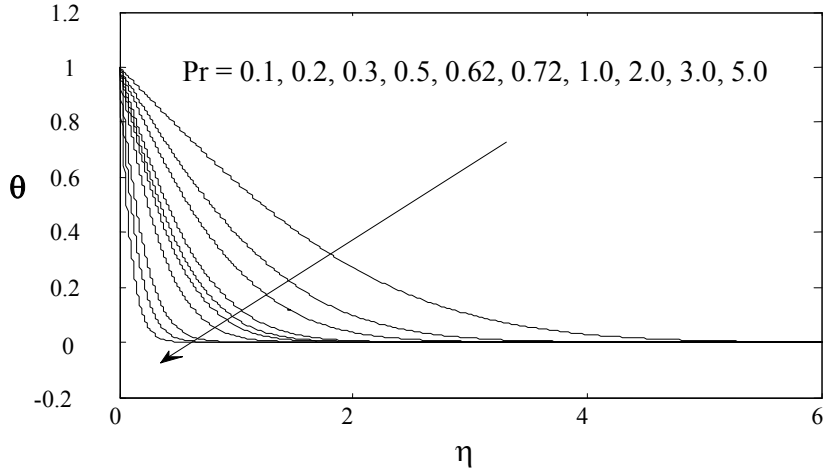

Figure 10 Effects of $\Pr$ on $\theta(\eta)$ at $\lambda = -2.0$, $M = 1.0$ $S = 2.0$, $\beta = 5.0$, $Ec = 0.1$, $A = 5.0$.

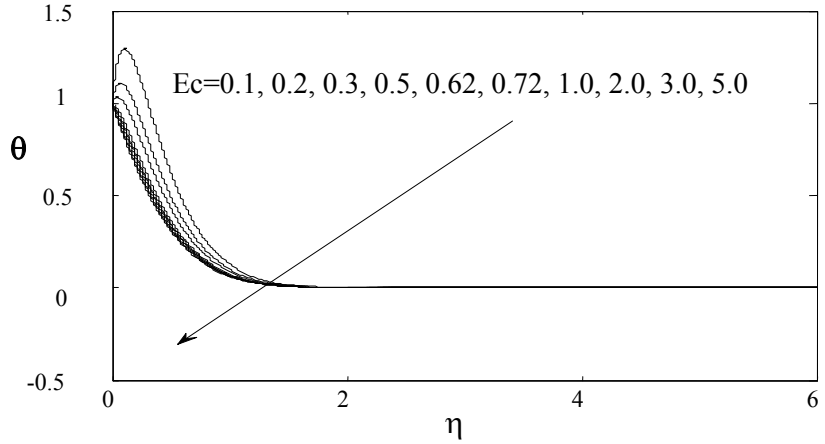

Figure 11 Effects of Ec on $\theta(\eta)$ at $M = 1.0$ $\beta = 5.0$, $\lambda = -2.0$, $A = 5.0$, $\Pr = 0.71$, $S = 2.0$.

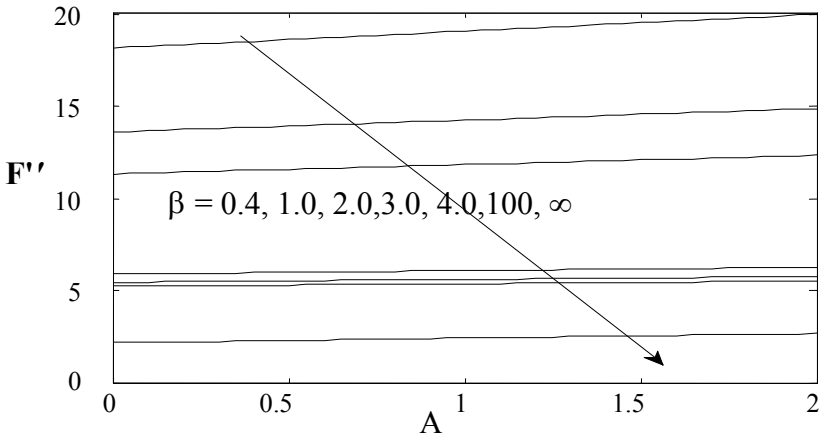

Figure 12 Effects of β on $f''(0)$ at $\lambda = -2.0$, $M = 1.0$ $S = 2.0$, $\Pr = 0.71$, $Ec = 0.1$, $A = 5.0$.

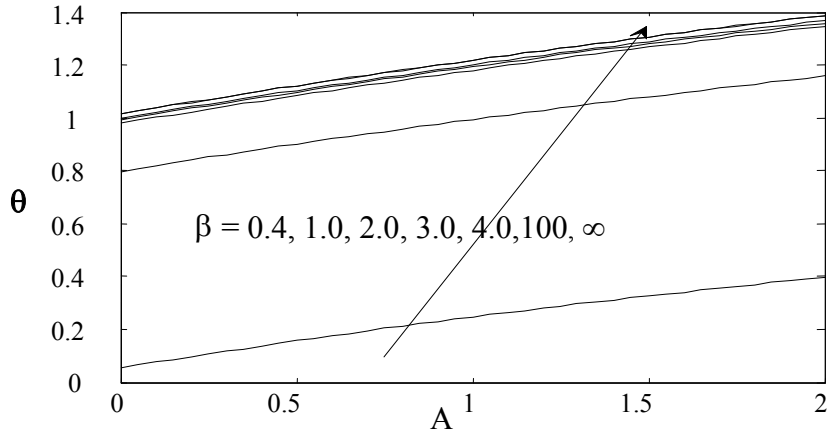

Figure 13 Effects of β on $\theta'(0)$ at $\lambda = -2.0$, $M = 1.0$ $S = 2.0$, $\Pr = 0.71$, $Ec = 0.1$, $A = 5.0$.

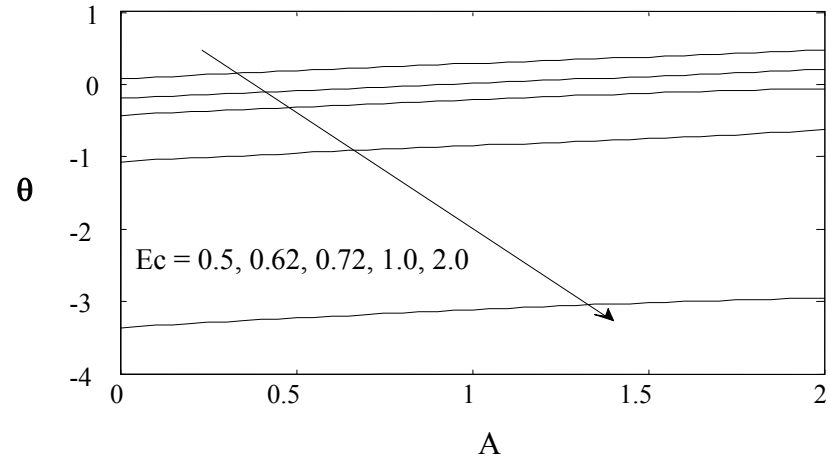

Figure 14 Effects of Ec on $\theta'(0)$ at $\lambda = -2.0$, $M = 1.0$, $S = 2.0$, $\beta = 5.0$, $Ec = 0.1$, $A = 5.0$.

It is noticed form **Figures 12** and **13** that the increase in Casson parameter β results in a decrease in $f''(0)$, whereas $\theta'(0)$ increases. Furthermore, $\theta'(0)$ increases with increase of the unsteadiness parameter A. **Figures 14** and **15** show that the heat transfer coefficient $\theta'(0)$ increases with increasing values of the Prandtl number Pr; however, it takes the opposite behavior with increase in Ec.

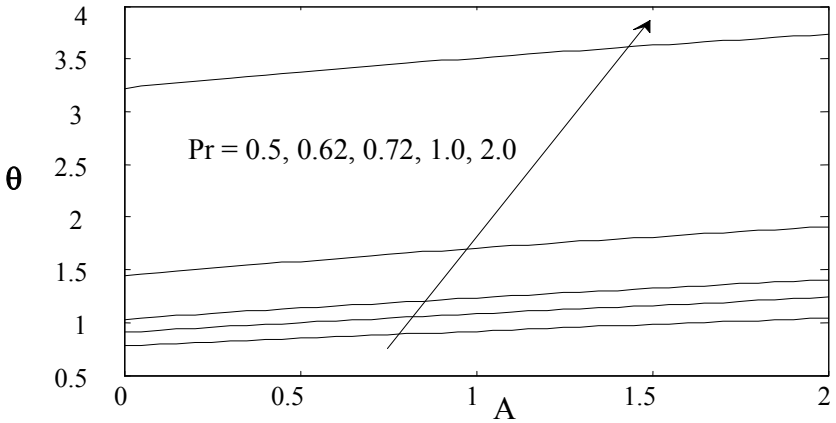

Figure 15 Effects of Pr on $\theta'(0)$ at $M = 1.0$, $\beta = 5.0$, $\lambda = -2.0$, $A = 5.0$, $\mathrm{Pr} = 0.71$, $S = 2.0$.

In addition, the influence of the suction parameter on the entropy generation number is shown in **Figure 16**. It is found that an increase in the suction parameter leads to an increase in the entropy generation. Moreover, the entropy generation number is higher near the surface, where both temperature and velocity take their maximum values. This means that the surface acts as a strong source of irreversibility. **Figure 17** illustrates the effect of the magnetic field parameter M on the entropy generation number. The entropy generation number takes its maximum at the higher values of magnetic

parameter. It can be concluded from this figure that the presence of the magnetic field helps in creating the entropy in the fluid.

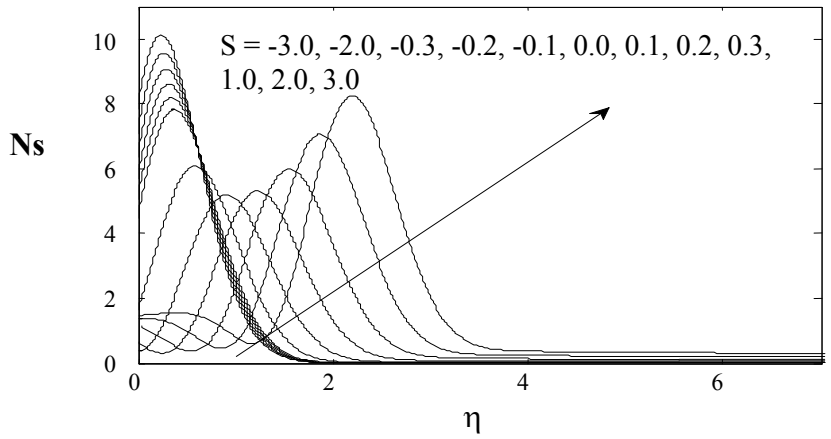

Figure 16 Effects of S on $Ns(\eta)$ at $\Pr = 0.71$, $M = 1.0$, $Ec = 0.1$, $\mathrm{Re}_l = 10.0$, $Br/\Omega = 0.2$.

Figure 18 shows the influence of the heat generation ($\lambda > 0$) or the heat absorption ($\lambda < 0$) parameter on the entropy generation number. As the heat source/sink parameter λ increases, the entropy generation number decreases. The effect of unsteadiness parameter A and Casson parameter β on the entropy generation number can be observed from **Figure**s **19** and **20**, respectively. As the unsteadiness parameter A and Casson parameter β increase, the entropy generation number increases. The influence of the Eckert number on the entropy generation number is shown in **Figure 21**. An increase of the Eckert number yields smaller entropy generation number. An augmentation of the Prandtl number, the dimensionless group parameter, and the Reynolds number results in higher entropy generation number, as can be noticed from **Figure**s **22 - 24**. In all cases, the surface acts as a strong source of irreversibility.

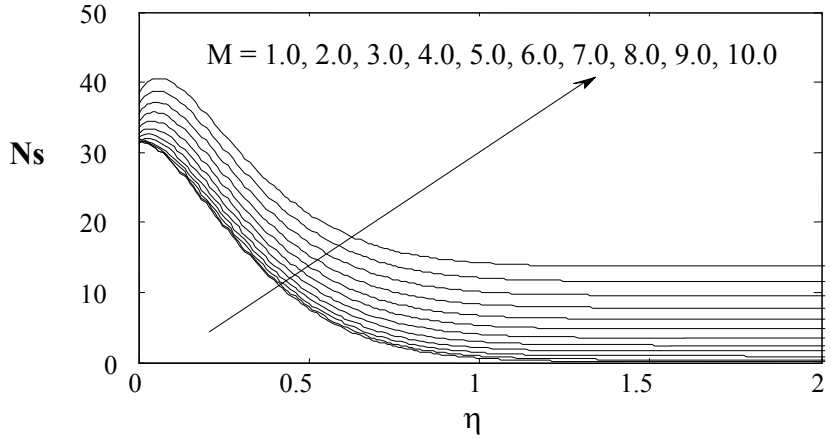

Figure 17 Effects of M on $Ns(\eta)$ at $\Pr = 0.71$, $M = 1.0$, $Ec = 0.1$, $\mathrm{Re}_l = 10.0$, $Br/\Omega = 0.2$.

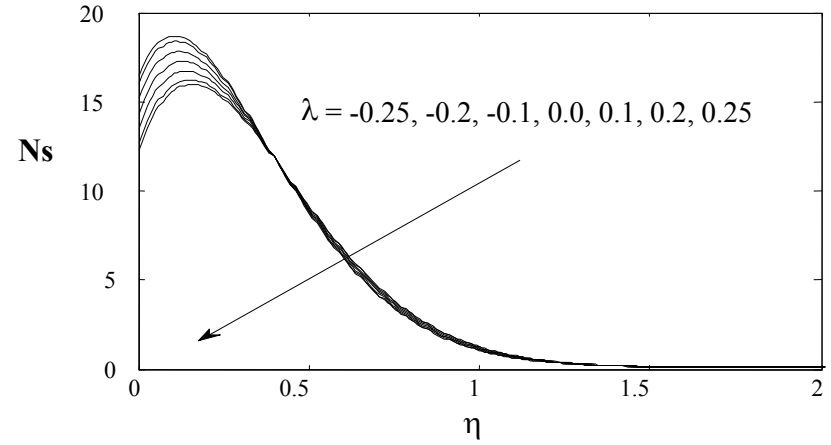

Figure 18 Effects of λ on $Ns(\eta)$ at $\Pr = 0.71,\ M = 1.0,\ Ec = 0.1,\ \mathrm{Re}_l = 10.0,\ Br/\Omega = 0.2.$

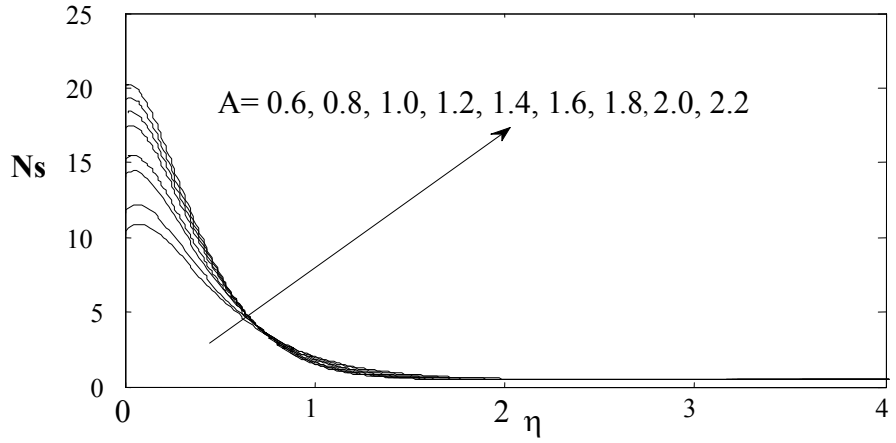

Figure 19 Effects of A on $Ns(\eta)$ at $\Pr = 0.71,\ M = 1.0,\ Ec = 0.1,\ \mathrm{Re}_l = 10.0,\ Br/\Omega = 0.2.$

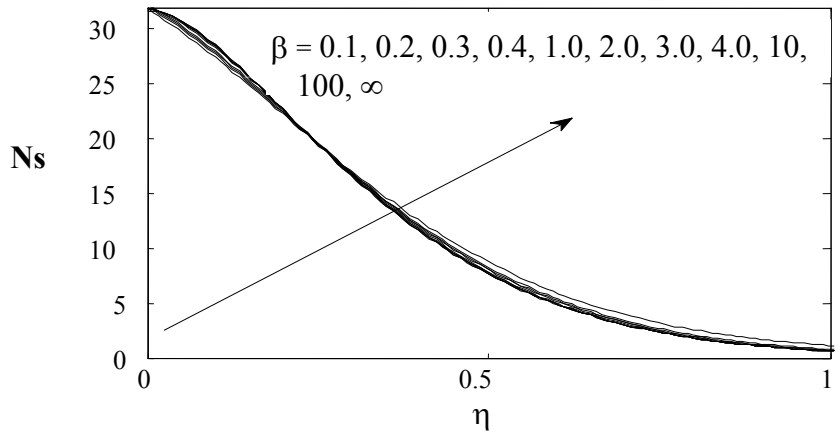

Figure 20 Effects of β on $Ns(\eta)$ at $\Pr = 0.71,\ M = 1.0,\ Ec = 0.1,\ \mathrm{Re}_l = 10.0,\ Br/\Omega = 0.2.$

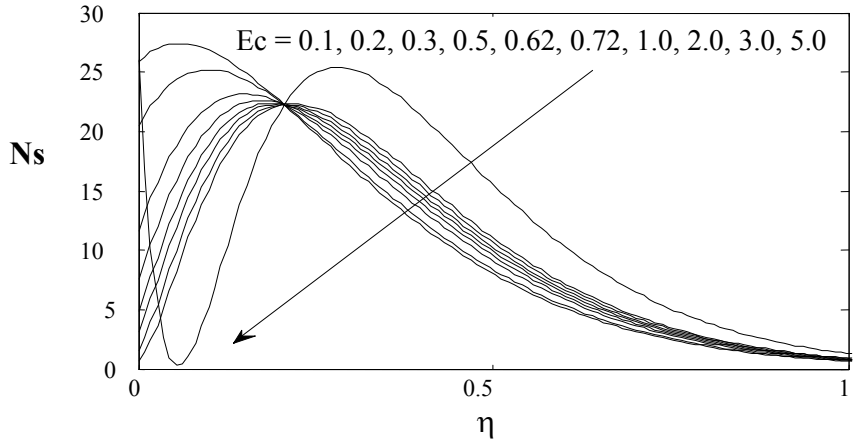

Figure 21 Effects of Ec on $Ns(\eta)$ at $\Pr = 0.71$, $M = 1.0$, $\mathrm{Re}_l = 10.0$, $Br/\Omega = 0.2$.

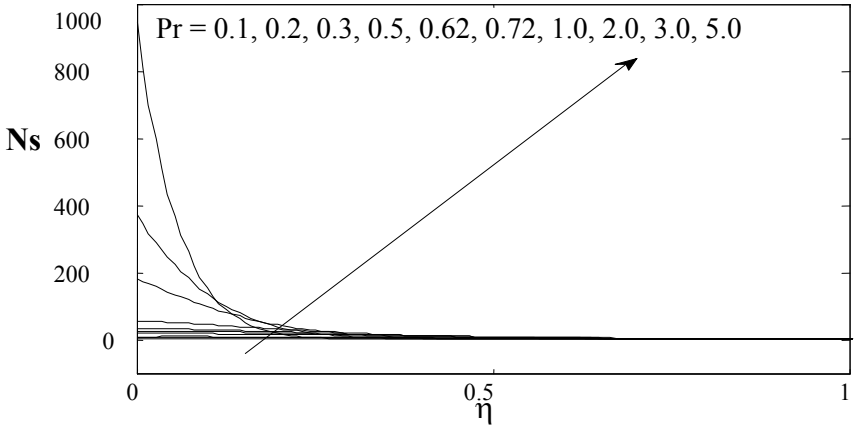

Figure 22 Effects of Pr on $Ns(\eta)$ at $M = 1.0$, $Ec = 0.1$, $\mathrm{Re}_l = 10.0$, $Be/\Omega = 0.2$.

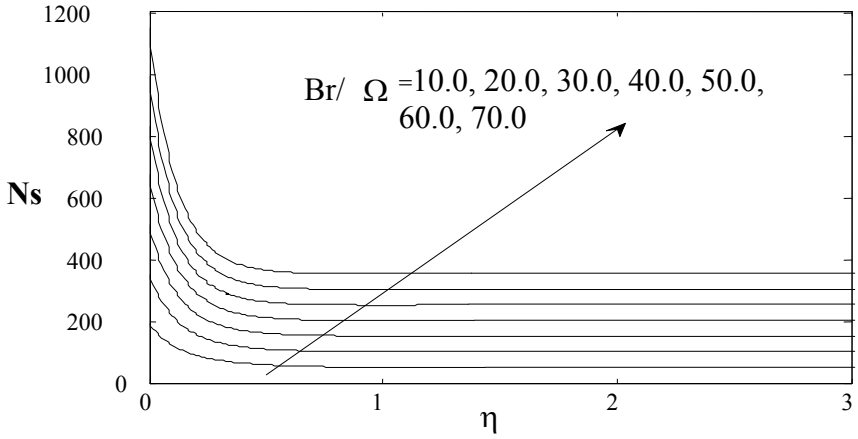

Figure 23 Effects of Be/Ω on $Ns(\eta)$ at $\Pr = 0.71$, $M = 1.0$, $\mathrm{Re}_l = 10.0$.

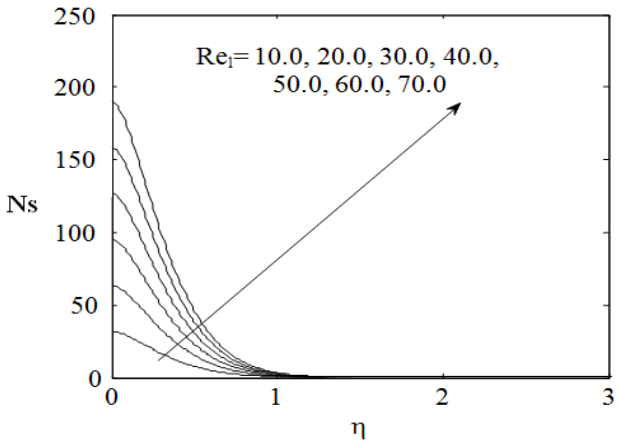

Figure 24 Effects of Re_l on $Ns(\eta)$ at $M = 1.0$, $Ec = 0.1$, $\mathrm{Pr} = 0.71$, $Br/\Omega = 0.2$.

Conclusions

In this study, the effects of unsteadiness parameter A on the entropy generation due to the boundary layer flow and heat transfer of a Casson fluid over a stretching sheet were investigated. The self similarity equations were obtained using suitable similarity transformations. The results of the problem show that, due to the increase of unsteady parameter A, Casson parameter β, magnetic field parameter M, and mass suction parameter S, the velocity profiles decreases. Also, the dimensionless temperature profile reduces as the Prandtl number increases. The thermal boundary layer thickness decreases as Eckert increases. For some higher values of the heat source\sink parameter λ occurring at the sheet, the velocity and temperature distributions decrease. The rate of heat transfer $\theta'(0)$ increases with increase of Casson parameter β, whereas the skin-friction $f''(0)$ takes the inverse behavior. The entropy generation number increases as the Prandtl number, magnetic parameter, surface temperature parameter, dimensionless group parameter, and Reynolds number increase. The entropy generation number is slightly positively influenced by the unsteadiness parameter, Casson parameter, and the heat source/ sink parameter. However, it decreases with the increase in Eckert number.

Acknowledgements

The authors of the paper would like to express their thanks for the referees for giving helpful suggestions, which led to the improvement in presentation.

References

[1] LJ Crane. Flow past a stretching plate. *Z. Angew. Math. Phys*. 1970; **21**, 645-7.
[2] B Sakiadis. Boundary layer behavior on continuous solid surfaces: I. Boundary layer equations for two dimensional and axisymmetric flow. *AIChE J*. 1961; **7**, 26-8.
[3] B Sakiadis. Boundary layer behavior on continuous solid surfaces: II. The boundary layer on a continuous flat surface. *AIChE J*. 1961; **7**, 221-5.
[4] L Howarth. *On the Calculation of Steady Flow in the Boundary Layer near the Surface of a Cylinder in a Stream*. H.M.S.O. Publisher, London, 1934.
[5] P Gupta and A Gupta. Heat and mass transfer on a stretching sheet with suction or blowing. *Can. J. Chem. Eng*. 1977; **55**, 744-6.
[6] C Wang. The three-dimensional flow due to a stretching flat surface. *Phys. Fluids* 1984; **27**, 1915-7.

[7] S Mishra and S Jena. Numerical solution of boundary layer MHD flow with viscous dissipation. *The Sci. World J*. 2014; **2014**, 756498.
[8] ME Ali and E Magyari. Unsteady fluid and heat flow induced by a submerged stretching surface while its steady motion is slowed down gradually. *Int. J. Heat Mass Trans.* 2007; **50**, 188-95.
[9] IH Andersson, JB Aarseth and BS Dandapat. Heat transfer in a liquid film on an unsteady stretching surface. *Int. J. Heat Mass Trans*. 2000; **43**, 69-74.
[10] BS Dandapat, B Santra and K Vajravelu. The effects of variable fluid properties and thermocapillarity on the flow of a thin film on an unsteady stretching sheet. *Int. J. Heat Mass Trans*. 2007; **50**, 991-6.
[11] E Elbashbeshy and M Bazid. Heat transfer over an unsteady stretching surface. *Heat Mass Trans.* 2004; **41**, 1-4.
[12] S Sharidan, T Mahmood and I Pop. Similarity solutions for the unsteady boundary layer flow and heat transfer due to a stretching sheet. *Int. J. Appl. Mech. Eng*. 2006; **11**, 647-54.
[13] A Ishak, R Nazar and I Pop. Heat transfer over an unsteady stretching permeable surface with prescribed wall temperature. *Nonlinear Anal. Real World Appl*. 2009; **10**, 2909-13.
[14] S Mukhopadhyay. Effect of thermal radiation on unsteady mixed convection flow and heat transfer over a porous stretching surface in porous medium. *Int. J. Heat Mass Trans*. 2009; **52**, 3261-5.
[15] S Mukhopadhyay. Effects of slip on unsteady mixed convective flow and heat transfer past a porous stretching surface. *Nucl. Eng. Des*. 2011; **241**, 2660-5.
[16] A Chamkha, AM Ali and MA Mansour. Similarity solution for unsteady heat and mass transfer from a stretching surface embedded in a porous medium with suction/injection and chemical reaction effects. *Chem. Eng. Commun.* 2010; **197**, 846-58.
[17] T Hayat and M Awais. Simultaneous effects of heat and mass transfer on time-dependent flow over a stretching surface. *Int. J. Numer. Meth. Fluids* 2011; **67**, 1341-57.
[18] S Mukhopadhyay and RSR Gorla. Unsteady MHD boundary layer flow of an upper convected Maxwell fluid past a stretching sheet with first order constructive/destructive chemical reaction. *J. Nav. Archit. Mar. Eng*. 2012; **9**, 123-33.
[19] T Hayat, M Awais, A Safdar and AA Hendi. Unsteady three dimensional flow of couple stress fluid over a stretching surface with chemical reaction. *Nonlinear Anal. Model. Control.* 2012; **17**, 47-59.
[20] T Hayat, SA Shehzad and A Alsaedi. Soret and Dufour effects on magnetohydrodynamic (MHD) flow of Casson fluid. *J. Appl. Math. Mech.* 2012; **33**, 1301-12.
[21] M Mustafa, T Hayat, I Pop and A Aziz. Unsteady boundary layer flow of a Casson fluid due to an impulsively started moving flat plate. *Heat Tran. Asian Res*. 2011; **40**, 563-76.
[22] S Mukhopadhyay, P Ranjan De, K Bhattacharyya and GC Layek. Casson fluid flow over an unsteady stretching surface. *Ain Shams Eng. J*. 2013; **4**, 933-8.
[23] K Bhattacharyya, T Hayat and A Alsaedi. Analytic solution for magnetohydrodynamic boundary layer flow of Casson fluid over a stretching/shrinking sheet with wall mass transfer. *Chin. Phys. B*. 2013; **22**, 024702.
[24] K Bhattacharyya, T Hayat and A Alsaedi. Exact solution for boundary layer flow of Casson fluid over a permeable stretching/shrinking sheet. *ZAMM Z. Angew. Math. Mech.* 2014; **94**, 522-8.
[25] M Qasim and S Noreen. Heat transfer in the boundary layer flow of a Casson fluid over a permeable shrinking sheet with viscous dissipation. *Eur. Phys. J. Plus*. 2014; **129**, 1-8.
[26] A Bejan. Second-law analysis in heat transfer and thermal design. *Adv. Heat Trans*. 1982; **15**, 1-58.
[27] A Bejan. Entropy generation minimization: The new thermodynamics of finite-size devices and finite-time processes. *J. Appl. Phys*. 1996; **79**, 1191-218.
[28] O Mahian, S Mahmud and S Z Heris. Analysis of entropy generation between co-rotating cylinders using nanofluids. *Energy* 2012; **44**, 438-46.
[29] HF Oztop and K Al-Salem. A review on entropy generation in natural and mixed convection heat transfer for energy systems. *Renew. Sust. Energ. Rev*. 2012; **16**, 911-20.
[30] S Aïboud and S Saouli. Second law analysis of viscoelastic fluid over a stretching sheet subject to a transverse magnetic field with heat and mass transfer. *Entropy* 2010; **12**, 1867-84.

[31] S Aïboud and S Saouli. Entropy analysis for viscoelastic magnetohydrodynamic flow over a stretching surface. *Int. J. Nonlinear Mech*. 2010; **45**, 482-9.
[32] M Govindaraju, NV Ganesh, B Ganga and AK Abdul Hakeem. Entropy generation analysis of magneto hydrodynamic flow of a nanofluid over a stretching sheet. *J. Egyptian Math. Soc.* 2015; **23**, 429-34.
[33] LC Woods. *The Thermodynamics of Fluid Systems*. Clarendon Press Oxford, 1975.
[34] MHAbolbashari, N Freidoonimehr, F Nazari and MM Rashidi. Entropy analysis for an unsteady MHD flow past a stretching permeable surface in nano-fluid. *Powder Technol*. 2014; **267**, 256-67.
[35] MM Rashidi, AB Parsa, L Shamekhi and E Momoniat. Entropy generation analysis of the revised Cheng-Minkowycz problem for natural convective boundary layer flow of nanofluid in a porous medium. *Therm. Sci*. 2015; **19**, S169-78.
[36] MM Rashidi, S Mahmud, N Freidoonimehr and B Rostami. Analysis of entropy generation in an MHD flow over a rotating porous disk with variable physical properties. *Int. J. Exergy* 2015; **16**, 481-503.
[37] MH Abolbashari, N Freidoonimehr, F Nazari and MM Rashidi. Analytical Modeling of Entropy Generation for Casson Nano-fluid Flow Induced by a Stretching Surface. *Adv. Powder Technol.* 2015; **26**, 542-52.